

THE MECHANISM OF QUARK CONFINEMENT

Gunnar S. Bali*

*Institut für Physik, Humboldt Universität, Invalidenstraße 110, 10115 Berlin,
Germany*

ABSTRACT

I summarise recent lattice results on the QCD confinement mechanism in the maximally Abelian projection.

1. Introduction

The phenomenology of strong interactions contains two fundamental ingredients: asymptotic freedom and the confinement of colour charges. The former requirement led to the invention of QCD. A mathematically rigorous proof that QCD as the *microscopic* theory of strong interactions indeed gives rise to the *macroscopic* property of linear quark confinement as indicated by Regg  trajectories and quarkonia spectra is, after a quarter of a century, still lacking. Meanwhile, lattice gauge theory simulations have provided convincing numerical evidence for this conjecture.

The difficulty in deriving infra red properties of QCD illustrates that something qualitatively new is happening: unlike in previously existing elementary physical theories, it is not possible to reduce everything down to two-body interactions but collective excitations of quark and gluon states have to be accounted for. For the first time, excitations of the vacuum that are considered to be fundamental do not occur as initial or final states anymore. Therefore, *understanding* confinement, in my opinion, is one of the most exciting challenges of modern physics. New physical and mathematical techniques that can successfully be applied to non-perturbative QCD might be required for dealing with other strongly interacting theories or theories with a non-trivial vacuum structure, in general. Vice versa techniques developed in a different context might help to prove QCD confinement and in solving QCD. A recent example is the proof of confinement in SUSY Yang-Mills theories.¹ Of course QCD as we know it does not obey super-symmetry but nonetheless such activities point into a promising direction. Just as QCD can serve as a guinea pig and development centre for non-perturbative techniques, lattice simulations help probing the validity range of effective low-energy models or in verifying certain conjectures.

QCD in itself is sufficiently complicated to keep many physicists busy. Solving QCD is still important and even more so since (almost) everyone believes in it. It is widely accepted that perturbative QCD (pQCD) successfully describes high energy scattering processes. However, without understanding non-perturbative aspects

*Talk given at 3rd International Conference on Quark Confinement and Hadron Spectrum (Confinement III), Newport News, VA, 7-12 Jun 1998.

of QCD, even in this case, it is not clear why pQCD works at all. Only hadrons, leptons and photons but no quarks or gluons are observed in experiment. In order to fill the gap, the formation of colour-neutral hadronic jets from quarks and gluons has to be modelled. Furthermore, it is commonly conjectured that, once the fundamental scattering on the quark and gluon level has taken place, further interactions can be neglected. It is demanding to derive the ingredients of fragmentation models directly from truly non-perturbative QCD, as well as to verify the factorisation hypothesis.

Many phenomenologically important questions are posed in low-energy QCD that eagerly await an answer: is the same set of fundamental parameters (QCD coupling and quark masses) that describes for instance the hadron spectrum consistent with high energy QCD or is there place for new physics? Are all hadronic states correctly classified by the naïve quark model or do glueballs, hybrid states and molecules play a rôle? At what temperatures/densities does the transition to a quark-gluon plasma occur? What are the experimental signatures of quark-gluon matter? Can we solve nuclear physics on the quark and gluon level? Clearly, complex systems like iron nuclei are unlikely ever to be solved from *first principles* alone but *modelling* and certain *approximations* will always be required. Therefore, it is desirable to test model assumptions, to gain control over approximations and, eventually, to derive low-energy effective Lagrangians from QCD. Lattice simulations are a very promising tool for this purpose.

In the past decades, many explanations of the confinement mechanism have been proposed, most of which share the feature that topological excitations of the vacuum play a major rôle. A list of these theories includes the dual superconductor picture of confinement,^{2,3} the centre vortex model,⁴ the instanton liquid model,⁵ and the anti-ferromagnetic vacuum.⁶ All these interpretations have been explored in lattice studies. The situation with respect to an anti-ferromagnetic vacuum is still somewhat inconclusive.⁷ Instantons seem to be more vital for chiral symmetry related properties than for confinement.⁸ Depending on the picture, the excitations giving rise to confinement are thought to be magnetic monopoles, instantons, dyons, centre vortices, etc.. I would like to stress that the above ideas are not completely disjoint and do not necessarily exclude each other. For instance, all the above mentioned topological excitations are found to be correlated with each other in numerical as well as analytical studies.

I will restrict myself to the, at present, most popular superconductor picture which is based on the concept of electro-magnetic duality after an Abelian gauge projection. Recently, the centre vortex model has been resuscitated too. In the latter picture, the centre group that is directly related to the traditional order parameter of the deconfinement phase transition in finite temperature pure gauge theories, the Polyakov line, plays an essential rôle. Another striking feature is that — unlike monopole currents — centre vortices form two-dimensional objects, such that in *four* space-time dimensions, a linking number between a Wegner-Wilson loop and centre vortices can unambiguously be defined, providing a geometric interpretation of the confinement mechanism.⁹ Unfortunately, I have not enough space to review these exciting developments. Therefore, I refer the interested reader to a review by Greensite.¹⁰

Another obvious omission are questions related to chiral properties of QCD. Real world QCD is not only a theory of gluons but includes quarks which means that the deconfinement phase transition will eventually be replaced by a chiral phase transition. In

the phase with broken chiral symmetry colour charges are still being anti-screened and linear confinement approximately holds. However, if the binding energy within a hadron exceeds a critical value, the hadron will break up into two or more colour-neutral parts (string breaking).

Based on different confinement pictures various effective models of infra red QCD have been proposed in the past. Three such examples are the Abelian Higgs model,^{11,9} the stochastic vacuum model¹² and dual QCD.¹³ As well as *understanding* the mechanism of confinement, it is desirable to verify aspects of these models and eventually to derive certain model parameters directly from QCD.

This article is organised as follows. I will start with a brief motivation and introduction into lattice methods in Sec. 2, before explaining the concept of the Abelian projection in Sec. 3. Subsequently, I will introduce some notations and review lattice results in Sec. 4 and conclude with a summary of answered and open questions.

2. Why Lattice?

Lattice methods allow for a somewhat *brute force* but *first principles* numerical evaluation of expectation values of a given quantum field theory that is defined by an action S . The lattice volume and spacing are limited due to finite computer speed and memory. Simulations are performed in Euclidean space and an analytic continuation to Minkowski space of numerical results that have been obtained on discrete points with finite precision is virtually impossible. Therefore, not every physically meaningful quantity can be calculated in a straight forward manner. The obvious strength of lattice methods are hadron mass determinations. Even if one is unimpressed by post-dictions of experimental values that have been known with high precision for decades, within an accuracy of only 5 %, such simulations allow one to fix fundamental standard model parameters like quark masses and QCD running coupling in the low-energy domain. Of course, plenty of other applications of phenomenological importance exist.

Unfortunately, only the lowest lying one or two radial excitations of a hadronic state are accessible in practice. Lattice predictions are restricted to rather simple systems too. Even the deuterium is beyond the reach of present day super-computers. Therefore, it is desirable to supplement lattice simulations by analytical methods. The computer alone acts as a *black box*. In order to understand and interpret the output values and to predict their dependence on the input parameters, some modelling is required. Vice versa, the lattice itself is a strong tool to validate models and approximations. Unlike in the “*real*” world, we can vary the quark masses m_q^i , the number of colours N_c , the number of flavours n_f , the temperature, the volume, the space-time dimension of our *femto*-universe and even the boundary conditions in order to expose models to thorough tests in many situations. Instead of indirectly and in a somewhat uncontrolled fashion deriving parameter values from experiment we can compute *custom designed* observables. What is thought to work in the real world ought to work on the lattice too! Moreover, many models rely on certain approximations. Experimentalists cannot switch off quark flavours but we can!

In a lattice simulation, hyper-cubic Euclidean space-time is discretised on a box with, say, L^4 lattice points or sites, x . Two adjacent points are connected by an oriented bond or link (x, μ) . The product of four links, enclosing an elementary square, is a

plaquette. Quarks are living on sites, gauge fields on links and the plaquette determines the curvature within the $SU(N_c)$ group manifold and corresponds to the field strength tensor. For simplicity, we assume an isotropic lattice with equal lattice spacing a in all directions. The lattice spacing provides an ultra violet cut-off on the gluon momenta $q < \pi/a$ and regulates the theory.

We simulate an action $S(\beta, m_q^i)$ on the lattice, which contains the quark masses as well as an inverse QCD coupling $\beta = 2N_c/g^2$ as free parameters. By varying β (and m_q^i) the lattice spacing a is changed. Asymptotic freedom tells us that the ultra violet cut-off is removed as $\beta \rightarrow \infty$. The physical dimension of a is determined by calculating a dimensionful quantity on the lattice and associating it to its experimental value. If the right theory is being simulated we should be able to reproduce all experimental mass ratios in the continuum limit $a \rightarrow 0$, such that it becomes irrelevant what experimental quantity we have chosen to set the scale*. In practice one does not get all the quark masses right, such that there are always systematic uncertainties in a , due to the ambiguity of the choice of this experimental input quantity.

The discretised lattice action is formulated in a manifestly gauge-invariant way and approaches the continuum action with $a \rightarrow 0$. One ideally extrapolates to this limit at fixed physical lattice extent, $La = \text{const.}$. Later on, the thermodynamic limit $La \rightarrow \infty$ should be investigated. Due to the finiteness of a computer these two extrapolations, as well as extrapolations and interpolations between results obtained at different quark masses, are subject to systematic uncertainties that have to be carefully estimated. For most hadronic processes, a lattice spacing $a < 0.1$ fm is considered to be *close* to the continuum limit while an extent $La \approx 2$ fm is comfortably large to accommodate ground state mesons and baryons.

Expectation values of operators O are determined by computation of the path integral,

$$\langle O \rangle = \frac{1}{Z} \int [dU][d\psi][d\bar{\psi}] O[U] e^{-S[U, \psi, \bar{\psi}]} \quad (1)$$

The normalisation factor Z is such that $\langle 1 \rangle = 1$. $U_{x,\mu} \in SU(N_c)$ denotes a gauge field and the $4 \times n_f \times N_c$ tuple ψ_x is a fermion field. The high-dimensional integral is evaluated by means of a (stochastic) Monte-Carlo method as an average over an ensemble of n *representative* gauge configurations, $\mathcal{C}_i = \{U_{x,\mu}^{(i)}\}, i = 1, \dots, n$. Therefore, the result on the expectation value is subject to a statistical error that will basically decrease like $1/\sqrt{n}$: the longer we *measure* the more precise the prediction becomes. Therefore, we might speak of *lattice measurements* and *lattice experiments* in analogy to “*real*” *experiments*. Ideally, the sample size n is such that the statistical precision is similar or smaller than the systematic uncertainty of the extrapolations.

In Fig. 1 I illustrate that confinement is a numerical fact by displaying the potential between a static quark and an anti-quark, separated by a distance r . The data have been obtained in $SU(3)$ gauge theory with and without two light (mass-degenerate)

*In the results presented here, I set the scale (somewhat arbitrarily) by the value $\sqrt{\sigma} = 440$ MeV for the string tension in case of $SU(2)$ and by the value $r_0 = 0.5$ fm in case of $SU(3)$ chromodynamics. r_0 is the distance at which $r_0^2 dV(r)/dr|_{r_0} = 1.65$ where $V(r)$ denotes the potential between two static colour sources, separated by a distance r .

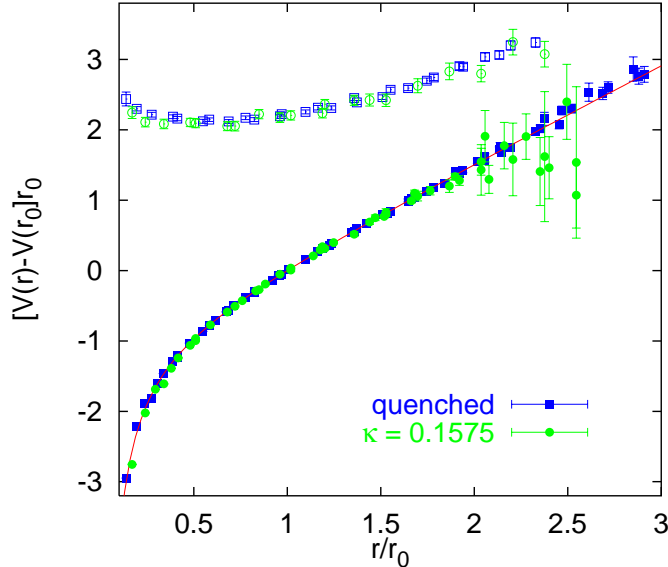


Fig. 1. Ground state (full symbols) and E_u hybrid potential (open symbols) at $\beta = 6.2$ (quenched) and $\beta = 5.6$, $\kappa = 0.1575$.¹⁴

quark flavours at lattice spacings somewhat smaller than 0.1 fm. The scale r_0 corresponds to 0.5 fm. The (partially) unquenched potential, that has been obtained at a quark mass $m_q \approx 50$ MeV, exhibits a more pronounced singularity at small r , due to the slower running of the QCD coupling towards *zero* as the momentum scale is increased (or r is decreased). Furthermore, from $r \approx 1.2$ fm onwards, the (partially) unquenched potential eventually flattens: the QCD string “breaks”. Indeed, many interesting features of the theory can be studied on the lattice that are not at all accessible to *real* experiment. As an example, I have included a so-called E_u (or continuum Π_u) hybrid potential^{15,16} into the plot that corresponds to the interaction energy of two static quark sources for the case that gluons contribute one unit of angular momentum along the interquark axis.

3. (Abelian) photons and monopoles

Soon after the advent of QCD, 't Hooft and Mandelstam² proposed the dual superconductor scenario of confinement; the QCD vacuum is thought to behave analogously to an electrodynamic superconductor but with the rôles of electric and magnetic fields being interchanged: a condensate of magnetic monopoles expels electric fields from the vacuum. If one now puts electric charge and anti-charge into this medium, the electric flux that forms between them will be squeezed into a thin, eventually string-like, Abrikosov-Nielsen-Olesen (ANO) vortex which results in linear confinement.

In all quantum field theories in which confinement has been proven, namely in compact $U(1)$ gauge theory in the Villain formulation,¹⁷ the Georgi-Glashow model¹⁸ and SUSY Yang-Mills theories,¹ this scenario is indeed realised. Before one can apply this picture to QCD or $SU(N_c)$ chromodynamics one has to identify the relevant dynamical variables: it is not straight forward to generalise the electro-magnetic duality of a $U(1)$ gauge theory to $SU(N_c)$ since gluons carry colour charges. How can

one define electric fields in a gauge invariant way? What fields are dual to the electric fields? How can one identify a monopole current? The next question is that for the order parameter of the confinement-deconfinement phase transition: what symmetry is broken? One might also ask why this symmetry is broken — a question that has been answered by the BCS theory for conventional superconductors. Finally, we are interested in an effective low-energy theory which corresponds to the Ginzburg-Landau theory of standard superconductors.

Let us address the first question. In the Georgi-Glashow model, the $SO(3)$ gauge symmetry is broken down to a $U(1)$ symmetry as the vacuum expectation value of the Higgs field becomes finite. Within this effective $U(1)$ theory, the standard electromagnetic duality is realised, resulting in confinement. Such a mechanism is not provided by QCD but one can attempt to reduce the $SU(N_c)$ symmetry to an Abelian symmetry *by hand*. In this spirit, it has been proposed³ to identify the monopoles in the $U(1)^{N_c-1}$ diagonal Cartan subgroup of $SU(N_c)$ gauge theory after gauge fixing in respect to the off-diagonal $SU(N_c)/U(1)^{N_c-1}$ degrees of freedom (Abelian projection).

In general, a gauge transformation, $\Omega_x \in SU(N_c)/U(1)^{N_c-1}$, can be found that diagonalises an arbitrary operator $X_x = f[U^\Omega]$ within the adjoint representation of $SU(N_c)$ when applied to the link variables,

$$U_{x,\mu}^\Omega = \Omega_x U_{x,\mu} \Omega_{x+a\hat{\mu}}^\dagger. \quad (2)$$

Subsequently, a coset decomposition of the gauge transformed links is performed,

$$U_{x,\mu}^\Omega = C_{x,\mu} u_{x,\mu} \quad \text{with} \quad C_{x,\mu} \in SU(N_c)/U(1)^{N_c-1}, \quad u_{x,\mu} \in U(1)^{N_c-1}. \quad (3)$$

If we now apply a residual gauge transformation, $\omega_x \in U(1)^{N_c-1}$, we find,

$$u_{x,\mu} \longrightarrow \omega_x u_{x,\mu} \omega_{x+a\hat{\mu}}^\dagger, \quad C_{x,\mu} \longrightarrow \omega_x C_{x,\mu} \omega_x^\dagger, \quad (4)$$

i.e. $u_{x,\mu}$ transforms like a gauge field while $C_{x,\mu}$ transform like matter fields. Therefore, we will refer to the diagonal gluon field $u_{x,\mu}$ as “photon” field. While the gauge fields of electrodynamics in the non-compact continuum formulation are free of singularities and, therefore, cannot form magnetic monopole solutions, the gauge transformation Ω_x is singular wherever two eigenvalues of X_x coincide. Therefore, the gauge field $u_{x,\mu}$ will in general contain such monopoles.

After Abelian gauge fixing QCD can be regarded as a theory of interacting photons, monopoles and matter fields (i.e. off-diagonal gluons and quarks). One might assume that the off-diagonal gluons do not affect long range interactions. This conjecture is known as *Abelian dominance*.¹⁹ In addition, *monopole dominance* of non-perturbative physics has been proposed.²⁰

The identification of photon fields and monopoles is a gauge invariant process. However, the choice of the operator X_x , that defines the Abelian projection, is ambiguous. In his original work, ‘t Hooft suggested that the dual superconductor scenario would be realised in any Abelian projection. Indeed, the expectation value of a monopole creation operator has been found to be an order parameter of the deconfinement phase transition in quite a few different projections of $SU(2)$ chromodynamics.²¹ As long as any $U(1)^{N_c-1}$ projection of the theory yields similar results, one

does not have to specify the mechanism that is thought to break the $SU(N_c)$ gauge symmetry of QCD. However, numerical simulations suggest that Abelian and monopole dominance are not at all universal. The most popular gauge projection applied and discussed is the maximally Abelian projection (MAP).³ One feature that is not shared by almost all other projections that have been investigated on the lattice so far is that the (local) MAP gauge condition gives rise to non-propagating ghost fields only, guaranteeing renormalisability of the Abelian projected theory. Another — and possibly related — fact is that both, Abelian and monopole dominance have qualitatively been verified in this projection.

One should mention that the analogy to an ordinary superconductor after Abelian projection is not complete. The electrons that form Cooper pairs in BCS theory are all negatively charged. However, the monopoles that are thought to condense in QCD can carry both, negative and positive magnetic charges. Therefore, the composition of the condensate is very different. The origin of the interaction that results in an attractive force between monopoles and anti-monopoles also differs from the periodic background potentials of the BCS theory.

I will briefly explain how MAP is performed on the lattice for the case of $SU(2)$ gauge theory. In the first step one maximises the functional,²²

$$F(\Omega) = \sum_{x,\mu} \text{tr} \left(\tau_3 U_{x,\mu}^\Omega \tau_3 U_{x,\mu}^{\Omega\dagger} \right), \quad (5)$$

by means of a gauge transformation Ω_x . τ_3 denotes a Pauli-matrix[†]. After the maximisation, all link variables are *as diagonal as possible*. The resulting gauge fields $U_{x,\mu}^\Omega = \exp \left(i \sum_c A_{x,\mu}^c \tau_c / 2 \right)$ satisfy 't Hooft's differential MA gauge fixing condition,³

$$\left(\partial_\mu \pm i A_{x,\mu}^3 \right) A_{x,\mu}^\pm = 0, \quad A_{x,\mu}^\pm = \frac{1}{\sqrt{2}} \left(A_{x,\mu}^1 \pm A_{x,\mu}^2 \right). \quad (6)$$

After gauge fixing, the projection is performed: observables are calculated on Abelian configurations $\{\theta_{x,\mu}\}$ rather than $\{U_{x,\mu}\}$. We refer to the field theory, defined in this way, as Abelian projected $SU(2)$ gauge theory [APSU(2)]. For convenience the Abelian links are represented in the Lie algebra rather than the group itself, $u_{x,\mu} = \exp(i\theta_{x,\mu}\tau_3)$. Note that the normalisation has been chosen such that the periodicity of θ_μ is 2π as opposed to the periodicity 4π of A_μ^3 . With this convention we find magnetic charges to be multiples of $2\pi/e$ just like in electrodynamics rather than $2N_c\pi/e$ as one might have expected in $SU(N_c)$ gauge theory. We also use the convention $e = 1$ for the fundamental electric charge.

Recently, some articles have appeared whose authors claim to have “proven” Abelian dominance, either in general or specifically in the MAP. In one case the argument is based on the fact that the off-diagonal gluon fields acquire mass and, therefore,

[†]In principle, we can fix the gauge along any direction within the $SU(2)$ group space. The resulting gauges will only differ from each other by a global gauge transformation that will not affect expectation values — as long as we perform the subsequent coset decomposition with respect to the same $U(1)$ subgroup. Also note that if we forced an adjoint Higgs field with a δ -like potential into the 3-direction, the form of the interaction term with the gauge fields would be identical to F .

are thought to affect ultra violet physics only, a statement that does not necessarily apply to confining field theories. Other arguments are either based on misinterpretations of the transfer matrix formalism or on rewriting the original theory in terms of Abelian projected variables plus perturbations (the off-diagonal fields) that are proportional to a *small* parameter ϵ . In order to avoid going too much into details I only mention that both, the static potential and Wilson loops in MAP are very different from their counter parts in the original theory, even for large distances. In case of the potential, the asymptotic slope (string tension) comes out to be similar. However, APSU(2) and $SU(2)$ potentials are shifted with respect to each other by a substantial constant due to different self-energy contributions. Any “*proof*” that fails to account for the latter fact is necessarily wrong to some extent.

4. Results

4.1. Some Definitions

The language of differential forms²³ turns out to be very convenient for the present purpose and this is even more so on the lattice. Let us start with a $U(1)$ field theory in $D = 4$ dimensions. The anti-symmetric field strength tensor F (a 2-form) can be decomposed as follows,

$$F = dA + \delta * C, \quad (7)$$

where A denotes the standard magnetic four-potential (1-form) and C denotes an electric four-potential which is a 1-form on the dual lattice. A and C are not uniquely determined but subject to a $U_{el}(1) \times U_{mag}(1)$ gauge invariance since gradients of scalar fields can be added. “ d ” denotes the exterior derivative that, applied to an n -form, results in an $n + 1$ -form. “ $*$ ” is the pull-back operator that connects an n -form to a $(D - n)$ -form on the dual lattice while the dual derivative $\delta = *d*$ turns n -forms into $(n - 1)$ -forms. We have $*^2 = 1$ and $d^2 = \delta^2 = 0$. We define a Laplacian $\square = (-)^D(d\delta + \delta d)$.

In this notation, we obtain the generalised Maxwell equations,

$$\delta F = j, \quad dF = *k. \quad (8)$$

The electric current j is a 1-form on the original lattice while the magnetic (monopole) current k is a 1-form on the dual lattice. In Landau gauge ($\delta A = 0$ or $\delta C = 0$, respectively) this means,

$$j = \square A, \quad k = \square C. \quad (9)$$

Note that, unlike the continuum four-potential A , the link angles $\theta \in (-\pi, \pi]$ are subject to a 2π shift-periodicity. Therefore, the identification,

$$F = \frac{1}{a^2} \sin(d\theta) \left[1 + \mathcal{O}(a^2) \right], \quad (10)$$

is natural for electro-magnetic fields. We can factorise the plaquette $d\theta \in (-4\pi, 4\pi]$ into a regular part $\bar{\theta}_{\square} \in (-\pi, \pi]$ and a singular part $m \in \{-2, -1, 0, 1, 2\}$:

$$d\theta = \bar{\theta}_{\square} + 2\pi m. \quad (11)$$

While $dd\theta = 0$, $d\bar{\theta}_\square = -2\pi dm$ does not necessarily vanish. Let us consider the magnetic flux through a (spatial) plaquette, $\Phi_{mag} = a^2 d\theta [1 + \mathcal{O}(a^2)]$, which, in the absence of monopole strings, would be identical to a contour integral of the vector potential A around the plaquette. However, in presence of monopoles, only $\exp(i \int_\square d^2 f d\theta) = \exp(i \int_{\partial\square} dx A)$ holds: the argument can be shifted by multiples of 2π which, with the normalisation $e = 1$, is the elementary monopole charge. Thus, $-2\pi m$ counts the monopole contribution to the magnetic flux through the plaquette and $-2\pi dm$ corresponds to the “flux” out of a 3-cube, such that²⁴

$$k = -2\pi *dm = *d\bar{\theta}_\square \quad (12)$$

is a magnetic monopole current[‡]. k is conserved since $\delta k = -2\pi\delta^2 *m = 0$, i.e. monopole currents form closed loops on the dual lattice. The individual components of k can take values $2\pi n$ with $n = -4, -3, \dots, 4$.

Monopole currents can alternatively be defined through,²⁵ $\tilde{k} = *dF = *d \sin(d\theta)$, the advantage being that the second Maxwell equation [Eq. (8)] is automatically fulfilled. The current \tilde{k} is obviously conserved too. The quantisation of magnetic charges, however, is obscured by lattice artefacts. Magnetic monopoles become extended objects and a geometric interpretation is not as straight forward as for the definition presented before. For all results I am going to review, the first definition has been used. Note that the locations of monopoles in either of the definitions are not necessarily identical to positions of singularities of the adjoint operator X that has been diagonalised by the gauge fixing, as originally proposed by 't Hooft.

Each link variable can be factorised^{26–28} into a *singular* part θ^{sing} that is induced by magnetic monopoles and a *regular* (or photon) part $\theta^{reg} = \theta - \theta^{sing}$ that obeys the homogenous Maxwell equation $dF = d \sin(d\theta^{reg}) = 0$. If we take the divergence of Eq. (11) in Landau gauge ($\delta\theta = 0$) we obtain,

$$2\pi\delta m = \delta d\theta = \square\theta^{sing}. \quad (13)$$

One solution of this equation is obviously,

$$\theta_x^{sing} = -2\pi \sum_y D_{xy} \delta m_y, \quad (14)$$

where D_{xy} denotes the lattice Coulomb propagator in position space.

Instead of using the Abelian links $\{\theta_{x,\mu}\}$ one can evaluate observables from the *monopole* and *photon* parts $\{\theta_{x,\mu}^{sing}\}$ and $\{\theta_{x,\mu}^{reg}\}$, separately. We will refer to such expectation values as *monopole* and *photon contributions*, respectively.

4.2. Successes

I will present some facts in support of the superconductor confinement scenario in the MAP: approximate Abelian dominance of the static potential has been verified.²⁰ In a recent study on a large lattice,²⁶ the APSU(2) string tension has been confirmed

[‡]I assume the quantities to be given in lattice units a . k has dimension a^{-3} , F has dimension a^{-2} .

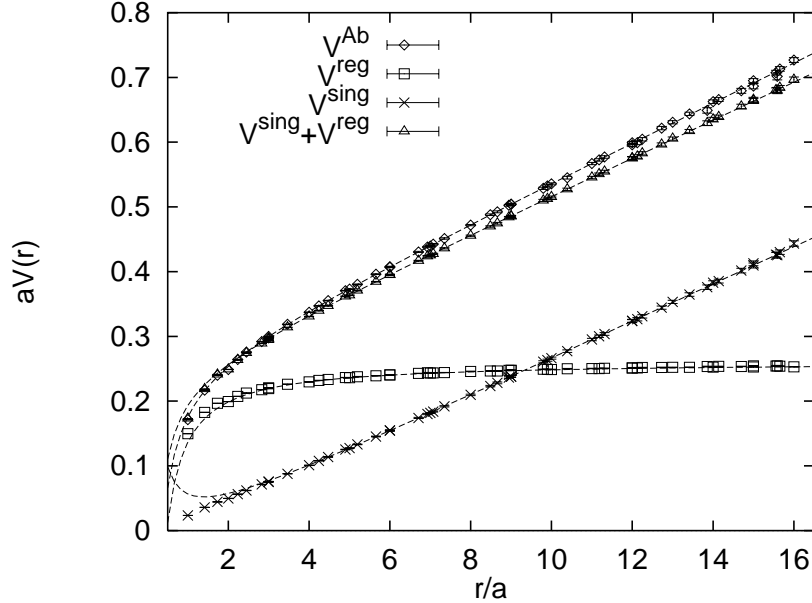


Fig. 2. Photon and monopole contributions V^{reg} and V^{sing} to the APSU(2) potential²⁶ V^{Ab} in units $a \approx 0.081$ fm.

to account for $(92 \pm 4)\%$ of the $SU(2)$ string tension. It is an open question whether the agreement will improve as the continuum limit is approached.

The photon part of the potential does not contain a linear contribution. Monopole dominance and the factorisation $V^{Ab}(r) = V^{sing}(r) + V^{reg}(r)$ approximately hold. In Fig. 2, we display the result of a recent lattice study.²⁶ Everything is plotted in lattice units $a \approx 0.081$ fm. The monopole contribution amounts to $(95 \pm 1)\%$ of the Abelian string tension.

Approximate Abelian and monopole dominance has been confirmed for the light hadron spectrum²⁹ of $SU(3)$ gauge theory. In Fig. 3, I display recent results on the nucleon and ρ masses that have been obtained on a lattice with extent $La \approx 2.8$ fm and spacing $a \approx 0.175$ fm. On the horizontal axis, the squared pion mass (in units of the string tension) is displayed, which changes as the quark mass is varied. Results for $SU(3)$, APSU(3) and Abelian monopole contributions as well as for $SU(3)$ with the photon part removed lie on the same curve. In the same study, π and ρ masses are found to become degenerate, as soon as the monopole contribution to the gauge fields is subtracted, both in $SU(3)$ chromodynamics and the Abelian projected theory, i.e. Abelian monopoles are required for chiral symmetry breaking. Consistent results have been found by Lee *et al.*²⁷ and Bielefeld *et al.*³⁰ Of course, one can also argue that since instantons are always accompanied by Abelian monopoles,³¹ removing these monopoles naturally results in a trivial vacuum topology.

The one-loop β -functions in APSU(N_c) and $SU(N_c)$ gauge theories agree,³² i.e. at weak coupling, masses obtained in both theories should be proportional to each other. A recent analytical investigation has also confirmed anti-screening of colour fields in APSU(2).³³ These results are in agreement with numerical data.^{26,34}

For the next few observations, I refer to M. Polikarpov's talk at this conference:

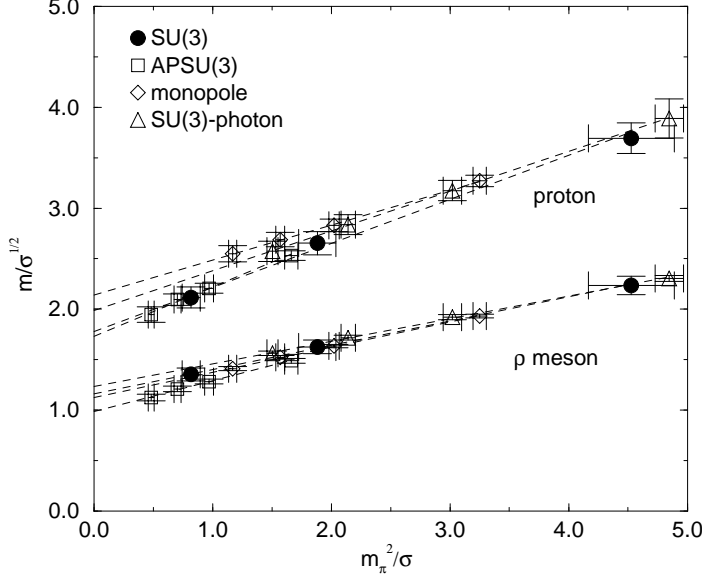


Fig. 3. $SU(3)$ ρ and nucleon masses: Abelian, monopole and non-photon contributions.²⁹

monopoles have been found to be condensed in the confined phase of $SU(2)$ gauge theory.^{21,35} Furthermore, APSU(2) monopoles are spatially correlated with regions of access in the $SU(2)$ action density³⁶ which rules out that the monopoles are mere gauge fixing artefacts since their presence is reflected in gauge invariant observables. An effective monopole Lagrangian has been constructed which can (approximately) be mapped onto the Abelian Higgs model.⁹

4.3. Puzzles

Of course, we do not expect $SU(N_c)$ gauge theories to be *identical* to an Abelian Higgs model. So, we should become suspicious if the picture did not fail to describe the QCD reality at some point. Obviously, APSU(2) becomes very different from $SU(2)$ gauge theory in the ultra violet. I will restrict myself to two points where something in the infra red might go wrong that I consider as being serious.

The static potential between sources within the adjoint representation of $SU(2)$ (adjoint potential) will saturate at a distance at which the binding energy exceeds the gluelump-gluelump threshold.¹⁵ Therefore, we expect for the adjoint string tension σ_{adj} the asymptotic value,

$$\sigma_{adj} = \lim_{r \rightarrow \infty} \frac{dV_{adj}(r)}{dr} = 0. \quad (15)$$

In APSU(2) we obtain for adjoint Wilson loops around a rectangle S ,

$$W_{adj}^{Ab}(S) = \frac{1}{3} [1 + 2W^{Ab,2}(S)], \quad W^{Ab,2} = \cos \left(2 \sum_{(x,\mu) \in \partial S} \theta_{x,\mu} \right), \quad (16)$$

where we call $W^{Ab,2}$ the *charge two* Wilson loop; the adjoint source corresponds to a *neutral* and two *charge two* Abelian components. Obviously, as the area S goes to

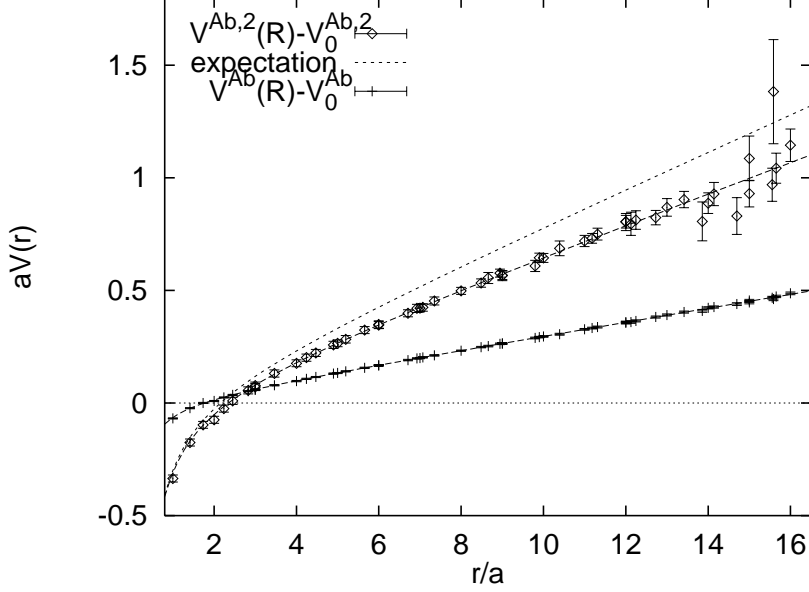


Fig. 4. The charge two potential in APSU(2) in lattice units $a \approx 0.081$ fm.²⁶

infinity, $W_{adj}^{Ab}(S)$ approaches the constant value $1/3$. Therefore,

$$V_{adj}^{Ab} = \frac{1}{a} \lim_{t \rightarrow \infty} \log \frac{W(r, t)}{W(r, t+a)} = 0 \quad \forall \quad r, \quad (17)$$

i.e. the correct asymptotic value $\sigma_{adj}^{Ab} = 0$ is produced.

However, lattice results indicate that the adjoint string will only break deep in the infra red at a distance slightly smaller than 1.5 fm,¹⁵ a region in which we would expect Abelian dominance to hold if we consider the MAP theory to have relevance for hadronic physics. Simple models predict a linear rise of the potential in the intermediate region, with a slope that is proportional to the Casimir charge of the representation, i.e. $\sigma_{adj} = 8/3 \sigma$ for $SU(2)$ gauge theory. Indeed, lattice simulations yield a linear increase, however with slightly smaller slope: $2\sigma \leq \sigma_{adj} < 8/3 \sigma$. In Fig. 4 the fundamental potential $V^{Ab}(r)$ is displayed, together with the *charge two* potential $V^{Ab,2}(r)$.²⁶ The curves are fits in accord to the parametrisation,

$$V^{Ab,(2)}(r) = -\frac{e^{Ab,(2)}}{r} + \sigma^{Ab,(2)} r. \quad (18)$$

The upmost curve corresponds to $e^{Ab,2} = 4e^{Ab}$, $\sigma^{Ab,2} = 8/3 \sigma^{Ab}$. As in $SU(2)$, we find the slope in APSU(2) to be somewhat smaller than expected.

In conclusion, it seems that the *charge two* potential resembles the features of the *adjoint* potential within $SU(2)$. However, it is not clear how we can get rid of the *neutral* contribution to the adjoint Wilson loop. For this purpose, interactions with the off-diagonal gluons have to be considered.

A second puzzle that has recently been noticed³⁴ is related to the energy distribution within the ANO vortex between static sources. In Fig. 5, I show the $1/e$

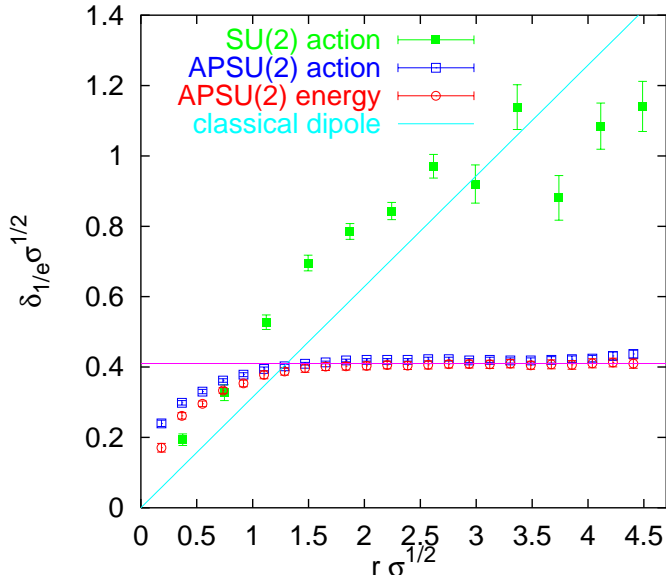


Fig. 5. $1/e$ -radius of the flux tube in $SU(2)$ and $APSU(2)$.³⁴

radius of the flux tube as a function of the source separation. The scale is set by $\sigma^{-1/2} \approx 0.45$ fm. In $SU(2)$ gauge theory only for the action density distribution a statistically reasonable signal has been obtained while for $APSU(2)$ we are able to display both, action and energy flux tube radii. While the width of the action density distribution in $SU(2)$ increases before it eventually saturates around a separation $r \approx 1.2$ fm at a value $2\delta_{1/e} \approx 0.9$ fm, both $APSU(2)$ widths become consistent with a constant $2\delta_{1/e} \approx 0.36$ fm as soon as $r > 0.5$ fm.

Obviously, the matter fields change the structure of the flux tube and, therefore, affect an infra red observable. However, only the shape differs while the cross section, i.e. the string tension, remains (almost) invariant. The tremendous width of the $SU(2)$ flux tube is somewhat counter-intuitive in view of the linear potential and the phenomenological success of string-like descriptions of hadrons; obviously, the $SU(2)$ flux tube is not one-dimensional and transverse degrees of freedom should be considered. However, the projected theory yields what we would have expected: a thin, string-like object. We might speculate that the Abelian projection reveals the physically relevant core of the vortex that becomes obscured by the matter fields of the full theory. However, we are left with a puzzle: why does the amplitude of the underlying transverse string fluctuations remain that constant? One should be able to reproduce such a vortex in terms of an effective string theory. The simplest such theories are not renormalisable in *four* dimensions. Therefore, the width should increase logarithmically with the rate being controlled by an ultra violet cut-off, i.e. the scale at which longitudinal fluctuations become important and the string description breaks down. This is obviously not the case for our $APSU(2)$ “string”. What is the physical mechanism that prevents the string from widening? Is the effective string theory supersymmetric³⁷? What correction terms have to be added in order to produce such a string?

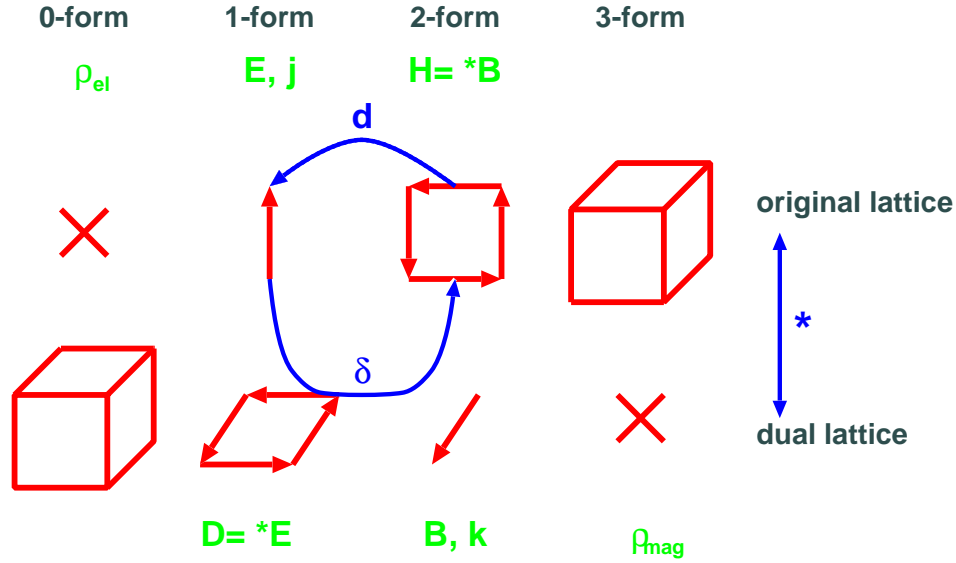


Fig. 6. Differential forms in $D = 3$ dimensions.

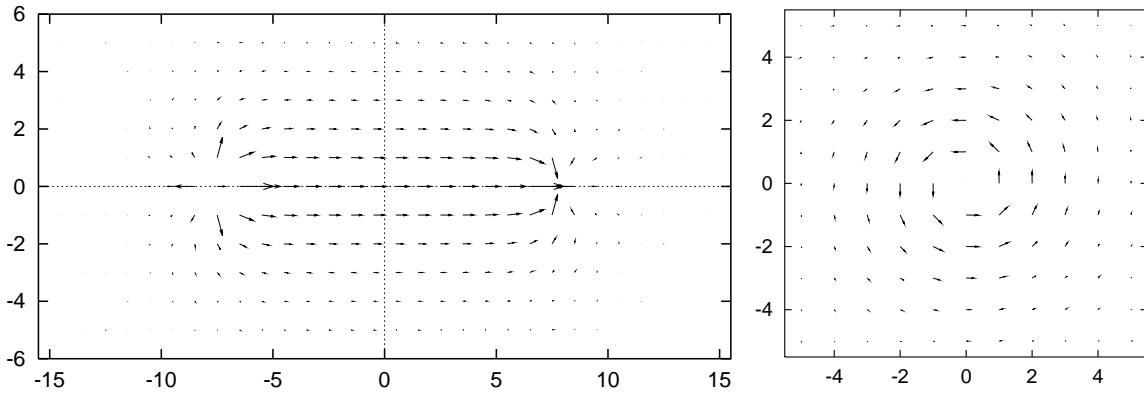


Fig. 7. Electric field \mathbf{E} and magnetic super current \mathbf{k} between two static sources.

4.4. The Dual Superconductor in Detail

In order to obtain an effective low-energy Lagrangian with monopoles and photons as fundamental degrees of freedom one can attempt to determine the free parameters by numerically matching the effective action to that of APSU(2).^{9,20} To complement such studies, one might probe the APSU(2) vacuum with electric (or magnetic) test charges to verify predictions of the effective theory and *measure* the values of the model parameters, which is the line I am going to follow here. Investigations of field distributions in presence of charges have been performed previously.³⁸ I will concentrate on the results from a more recent study.³⁹

We are probing the vacuum with *static* electric sources. For this purpose we consider three dimensional spatial cross sections (time slices) of the lattice. In Fig. 6, I have visualised where on the lattice different objects are “living”. The advantage in working with differential forms is that the Stokes theorem is guaranteed to be exact and not subject to lattice artefacts: if the differential Maxwell equations are fulfilled,

the integrated versions automatically hold too. Of course, when finally relating lattice results to continuum physics, lattice artefacts re-enter the game. The (generalised) Maxwell equations [Eq. (8)] read,

$$\delta\mathbf{E} = \rho_{el}, \quad d\mathbf{E} = *\mathbf{k} - *\dot{\mathbf{B}}, \quad (19)$$

$$\delta\mathbf{B} = \rho_{mag}, \quad d\mathbf{B} = *\mathbf{j} + *\dot{\mathbf{E}}. \quad (20)$$

The charge densities ρ_{el} and ρ_{mag} are the 4-components of j and k , respectively. The “*dof*”-symbol denotes a temporal derivative. For a static problem, electric and magnetic fields decouple. In the absence of magnetic test charges, this implies $\rho_{mag} = 0$, $\mathbf{j} = \mathbf{0}$ and, therefore, $\mathbf{B} = \mathbf{0}$ such that we are left with two Maxwell equations only, $\delta\mathbf{E} = \rho_{el}$ and $d\mathbf{E} = *\mathbf{k}$.

As mentioned above, one can define the monopole current via the latter equation (Ampère’s law) which is then trivially fulfilled. However, with our definition of \mathbf{k} [Eq. (12)] neither of the equations necessarily holds. Strong fields may give rise to non-linear quantum corrections. Moreover, APSU(2) is not electrodynamics; in general, the action will be non-local and the equations of motion might differ. Our numerical study, however, verifies $\text{div } \mathbf{E}$ to disappear outside of the vicinity of the sources while the curl of the electric field is identical to the magnetic current.³⁹ I display the electric field for a distance $r = 15a \approx 1.2$ fm in Fig. 7. The vortex is stabilised by the surrounding super current \mathbf{k} .

The starting point of our investigation is the London limit. The electric vector potential \mathbf{C} on the dual lattice is defined through,

$$\mathbf{E} = *d\mathbf{C}. \quad (21)$$

One representation of the (dual) London equations reads,

$$\mathbf{C} + \lambda^2\mathbf{k} = 0, \quad (22)$$

with λ being the inverse mass of the dual photon. By building the curl of this relation, we obtain $\mathbf{E} = -\lambda^2 *d\mathbf{k}$ which, together with the dual Ampère law results in,

$$\mathbf{E} = -\lambda^2\delta d\mathbf{E} = \lambda^2(\nabla^2\mathbf{E} + d\rho_{el}). \quad (23)$$

Without an electric current \mathbf{j} , the Maxwell equations imply, $d(\mathbf{B} + \lambda^2d\mathbf{k}) = 0$, i.e. even in the absence of a magnetic field, the super current \mathbf{k} remains constant and in general non-*zero*. From Eq. (23) it is also obvious why λ is called the *penetration length*: if we expose a superconducting probe to a homogeneous electric field, $\mathbf{E} = E_z\mathbf{e}_z$, the field strength will decay with the distance x towards the centre of the medium: $E_z(x) = E_z(0)\exp(-x/\lambda)$.

We create a charge-anticharge pair at a separation r parallel to the z -axis of our lattice, $\rho_{el} = \delta^3(-r/2\mathbf{e}_z) - \delta^3(r/2\mathbf{e}_z)$. x denotes the transverse distance from the core of the ANO vortex. For the electric flux through any surface enclosing the charge, we expect $\Phi_{el} = \int d^2x E_z(x, 0) = 1$. For our geometry Eq. (23) reads in the centre plane perpendicular to the vortex,

$$E_z(x) = \lambda^2\nabla_2^2 E_z(x) + \Phi\delta^2(x), \quad E_x(x) = 0. \quad (24)$$

A solution can be expressed in terms of the modified Bessel function K_0 ,

$$E_z(x) = \frac{\Phi_{el}}{2\pi\lambda^2} K_0(x/\lambda). \quad (25)$$

Within statistical accuracy, we find our data to be compatible with such a functional form for $x > x_{\min} = 4.2a \approx 0.35 \text{ fm}^{\S}$ with parameter values,

$$\lambda = (1.82 \pm 0.07)a \approx (1.3 \text{ GeV})^{-1}, \quad \Phi_{el} = 1.44 \pm 0.08. \quad (26)$$

For small x the data are overestimated by the fit since $K_0(x)$ diverges as $x \rightarrow 0$ which explains why the electric flux comes out to be significantly larger than *one*. A dual photon mass of 1.3 GeV is compatible with the mass of the lightest glueball in $SU(2)$ gauge theory. However, the quantum numbers of a dual photon are $J^{PC} = 1^{+-}$ as opposed to 0^+ for this glueball.

How can we refine our description such that the electric field not only in the surface region but also closer to the centre of the vortex is correctly reproduced? Obviously, a second scale ξ that is smaller than the 0.035 fm, above which the London limit seems to apply, has to be introduced. Such a scale appears in the Ginzburg-Landau (GL) equations as the *coherence length* of the GL wave function $\psi(\mathbf{x})$ that describes the spatial density of superconducting monopole charges, $n(\mathbf{x}) = |\psi(\mathbf{x})|^2$. We decompose ψ into a phase and an amplitude f ,

$$\psi(\mathbf{x}) = \psi_{\infty} f(\mathbf{x}) e^{i\theta(\mathbf{x})}, \quad f(\mathbf{x}) \xrightarrow{x \rightarrow \infty} 1. \quad (27)$$

ξ characterises the decay of the monopole density towards the centre of the vortex, where f will vanish as superconductivity breaks down, while λ controls the penetration of the vortex field into the surrounding vacuum. The case $\xi = 0$ corresponds to the London limit. If we increase the width of the flux tube, the dia-electric energy of the vortex is reduced by an amount roughly in proportion to λE^2 while the amount of energy we have to pay for pushing the monopoles further into the vacuum increases like ξE^2 . Values $\xi < \sqrt{2}\lambda$ correspond to a negative surface energy in accord to the Abrikosov criterium for a classical system. This tendency to maximise the surface results in retardation of flux tubes: we obtain a type II superconductor while values $\kappa = \lambda/\xi < 1/\sqrt{2}$ correspond to a type I superconductor. From our experience we are prejudiced to expect a type II scenario since in electrodynamics type I flux tubes cannot be realised due to the absence of isolated magnetic charges. In the present situation, however, the presence of two isolated electric sources forces the field lines through the surrounding vacuum, regardless of the type of the superconductor.

If we restrict ourselves to the perpendicular centre plane, the equation $d\mathbf{C} = *\mathbf{E}$ implies for the azimuthal component of \mathbf{C} (up to gauge transformations),

$$C_{\theta}(x) = \frac{1}{2\pi x} \int_{x' < x} d^2x' E_z(x') \xrightarrow{x \rightarrow \infty} \frac{\Phi_{el}}{2\pi x}, \quad (28)$$

[§] Along off-axis lattice directions, we obtain data for non-integer multiples of the lattice spacing.

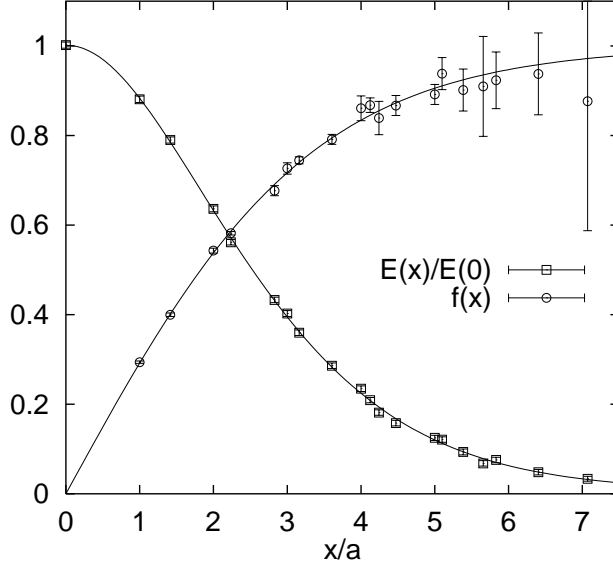


Fig. 8. The electric field and the amplitude of the Ginzburg-Landau wave function against the distance from the centre of the ANO vortex.³⁹

while the other components vanish. For non-constant density of magnetic charges, the London equation Eq. (22) is modified and becomes the second GL equation,

$$\left(C_\theta(x) - \frac{\Phi_{el}}{2\pi x}\right) + \frac{\lambda^2}{f^2(x)}k_\theta(x) = 0. \quad (29)$$

We can solve this equation with respect to $F(x) = f(x)/\lambda$ after having reconstructed $C_\theta(x)$ via Eq. (28).

The result is displayed in Fig. 8, together with $E_z(x)$. Data obtained at $x < 2.2a$ has to be treated with care since the difference between lattice and continuum versions of “curl” turns out to be bigger than our statistical uncertainty. For $x > 4.2a$ the errors on f explode: here, no contradiction to the London limit has been found. We fit $F(x)$ with the ansatz,

$$F(x) = \frac{f(x)}{\lambda} = \frac{1}{\lambda} \tanh(x/\alpha), \quad (30)$$

which conforms to the right boundary conditions. The fit is included into the figure as well as the result of a fit of E_z to a more involved four parameter ansatz that also respects the boundary conditions on f .³⁹ From the fit Eq. (30) we obtain $\lambda = 1.62(2)a$. The fit to E_z yields $\lambda = 1.84(8)a$ while a simultaneous fit to E_z and k_θ yields $\lambda = 1.99(5)a$. This has to be compared with the value $\lambda = 1.82(7)a$ from the London limit fit of Eq. (25). We end up with the conservative estimate,

$$\lambda = 1.84_{-24}^{+20}a = (0.15 \pm 0.02) \text{ fm}, \quad \Phi_{el} = 1.08 \pm 0.02. \quad (31)$$

One should settle in a scaling study whether the deviation from $\Phi_{el} = 1$ can be attributed to a non-trivial vacuum dielectricity constant due to anti-screening.

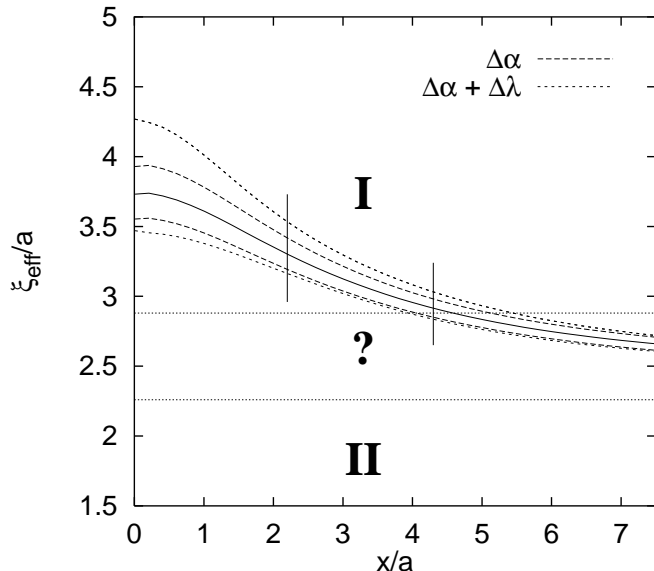


Fig. 9. Effective coherence length versus distance from the centre of the ANO vertex.³⁹

Since the first GL equation is non-linear, we cannot consistently formulate it in terms of differential forms on a lattice, i.e. — unlike the Maxwell equations — we have to verify it in the *continuum* and discard data obtained at small x/a values where the lattice structure is still apparent. For our geometry the first GL equation reads,

$$f(x) = f^3(x) + \xi^2 h(x) \left\{ \left[\frac{1}{x} - \frac{2\pi C_\theta(x)}{\Phi_{el}} \right]^2 - \frac{1}{x} \frac{d}{dx} \left(x \frac{d}{dx} \right) \right\} f(x). \quad (32)$$

Our strategy is to solve this equation with respect to an *effective* coherence length $\xi_{\text{eff}}(x)$, employing the above mentioned parametrisations of $E_z(x)$ and $f(x)$ to interpolate the data. The result is visualised in Fig. 9. Results outside of the window of observation $2.2 < x/a < 4.2$ are unreliable, for small x due to lattice artefacts and for large x due to lacking precision data on f . The figure contains error bands that are related to the uncertainties in α as well as in λ . Within the window, ξ_{eff} varies by only 10 %, i.e. the GL equation is qualitatively satisfied. Taking this variation of ξ with x into account, we obtain the result,

$$\xi = 3.10_{-35}^{+43} a = (0.251 \pm 0.032) \text{ fm}. \quad (33)$$

The central value corresponds to $\xi = \xi_{\text{eff}}(\xi)$.

For the ratio of penetration and coherence lengths we determine,

$$\kappa = 0.59_{-14}^{+13} < \frac{1}{\sqrt{2}}, \quad (34)$$

i.e. we have evidence of a *weak* type I superconductor. However, we are rather close to the Abrikosov limit whose position might differ from $1/\sqrt{2}$ due to quantum corrections.

In order to finally settle the question of the type of the superconductor, interactions between two flux tubes should be investigated. This has been done in recent studies of the confined phase of $U(1)$ gauge theory⁴⁰ as well as in three-dimensional Z_2 gauge theory,⁴¹ the result being attraction in both cases, i.e. type I superconductivity.

5. Summary and Open Questions

The lattice is an ideal tool to test ideas on the confinement mechanism. Many infra red aspects of QCD are reproduced in the maximally Abelian projection. After the projection only the monopole contribution to the original gauge fields seems to be relevant for most low-energy properties. The dual Maxwell equations have been verified in APSU(2) and the fields are adequately described by the dual Ginzburg-Landau equations with the values $\lambda = 0.15(2)$ fm and $\xi = 0.25(3)$ fm for penetration and coherence length, respectively. These values correspond to a (dual) photon mass $m_\gamma \approx 1.3$ GeV $\approx 3\sigma$ and a Higgs mass of $m_H \approx 0.8$ GeV $\approx 2\sigma$, the ratio of which, $\kappa = \lambda/\xi = 0.59(13)$, indicates the vacuum of $SU(2)$ gauge theory to be a (weak) type I superconductor. It is demanding to clarify whether flux tubes in $SU(N_c)$ gauge theory as well as in the Abelian projected theory attract or repel each other.

Electric flux tubes are found to be significantly thinner after the Abelian projection. Contrary to $SU(2)$ gauge theory, their width seems to saturate at a separation $r \approx 0.5$ fm at a value, $2\delta_{1/e} \approx 0.36$ fm. The Abelian projection also seems to suffer under problems with charges in non-fundamental representations. These observations require further thought. In the end we would like to clarify the rôle that charged gluons play. Ideally, one would like to completely circumvent the Abelian projection and arrive at a genuinely non-Abelian description of the superconductor scenario. In view of the existence of other reasonable proposals for the confinement mechanism more thought should be spend on relations between different such pictures.

An extension of the detailed superconductor study presented from $SU(2)$ to $SU(3)$ gauge theory should be attempted. It is interesting to simulate the 4D Abelian Higgs model with the m_γ and m_H parameters that have been predicted above and compare the resulting flux distributions with the result from APSU(2). This approach has recently been pursued by Chernodub and collaborators.⁹

Acknowledgements

This work has been supported by DFG grant Ba 1564/3. I thank my collaborators, in particular V. Bornyakov, M. Müller-Preußker, K. Schilling, and C. Schlichter.

References

1. N. Seiberg and E. Witten, Nucl. Phys. **B426**, 19 (1994).
2. G. 't Hooft, in *High Energy Physics*, ed. A. Zichici (Editrice Compositori, Bologna, 1976); S. Mandelstam, Phys. Rept. C **23**, 245 (1976).
3. G. 't Hooft, Nucl. Phys. **B190**, 455 (1981).
4. J. Ambjorn and P. Oleson, Nucl. Phys. **B170**, 265 (1980).
5. D.I. Diakonov and V.Yu. Petrov, Nucl. Phys. **B245**, 259 (1984).
6. G.K. Savvidy, Phys. Lett. **71B**, 133 (1977).

7. P. Cea and L. Cosmai, Phys. Rev. D **43**, 620 (1991); H.D. Trottier and R.M. Woloshyn, Phys. Rev. Lett. **70**, 2053 (1993).
8. See e.g., J.W. Negele, hep-lat/9804017.
9. M. Polikarpov, *Proc. Confinement III*, TJ Lab., 1998.
10. L. Del Debbio, M. Faber, J. Giedt, J. Greensite, and S. Olejnik, hep-lat/9801027 and references therein.
11. T. Suzuki, Prog. Theor. Phys. **80**, 929 (1988).
12. H.G. Dosch, *Proc. Confinement III*, TJ Lab., 1998.
13. M. Baker, *Proc. Confinement III*, TJ Lab., 1998.
14. $T\chi L$ collaboration: G.S. Bali *et al.*, in preparation.
15. C. Michael, *Proc. Confinement III*, TJ Lab., 1998, hep-lat/9809211.
16. C. Morningstar, *Proc. Confinement III*, TJ Lab., 1998, hep-lat/9809305; J.E. Paton, *ibid.*; T.J Allen, *ibid.*
17. T. Banks, R. Myerson, and J. Kogut, Nucl. Phys. **B129**, 493 (1977).
18. A.M. Polyakov, JETP Lett. **20**, 194 (1974); G. 't Hooft, Nucl. Phys. **B79**, 276 (1974).
19. Z.F. Ezawa and A. Iwazaki, Phys. Rev. D **25**, 2681 (1982).
20. See e.g., T. Suzuki, Prog. Theor. Phys. Suppl. **122**, 75 (1996).
21. See e.g., A. Di Giacomo, hep-th/9809047.
22. A.S. Kronfeld, G. Schierholz, U.-J. Wiese, Nucl. Phys. **B293**, 461 (1987).
23. See e.g., P. Becher and H. Joos, Zeit. Phys. **C15**, 343 (1982).
24. T.A. DeGrand and D. Toussaint, Phys. Rev. D **22**, 2478 (1980).
25. M. Zach, M. Faber, W. Kainz and P. Skala, Phys. Lett. **B358**, 325 (1995).
26. G.S. Bali, V. Bornyakov, M. Müller-Preußker, and K. Schilling, Phys. Rev. D **54**, 2863 (1996).
27. F.X. Lee, R.M. Woloshyn, and H.D. Trottier, Phys. Rev. D **53**, 1532 (1996).
28. J. Smit and A.J. van der Sijs, Nucl. Phys. **B355**, 603 (1991).
29. S. Kitahara *et al.*, hep-lat/9803020.
30. T. Bielefeld, S. Hands, J. Stack, J. Wensley, Phys. Lett. **B415**, 150 (1998).
31. V. Bornyakov and G. Schierholz, Phys. Lett. **B384**, 190 (1996); A. Hart and M. Teper, Phys. Lett. **B371**, 261 (1996); H. Suganuma, K. Itakura, H. Toki, and O. Miyamura, hep-ph/9512347.
32. M. Quandt and H. Reinhardt, Phys. Lett. **B424**, 115 (1998); K.-I. Kendo, *Proc. Confinement III*, TJ Lab., 1998, hep-th/9808186.
33. G. Di Cecio, A. Hart, and R.W. Haymaker, hep-lat/9807001.
34. G.S. Bali, K. Schilling, and C. Schlichter, in preparation.
35. M. Chernodub, M. Polikarpov, A. Veselov, Phys. Lett. **B399**, 267 (1997).
36. B.L.G. Bakker, M.N. Chernodub, and M.I. Polikarpov, Phys. Rev. Lett. **80**, 30 (1998); E.-M. Ilgenfritz, H. Markum, M. Müller-Preußker, and S. Thurner, hep-lat/9801040.
37. J. Greensite and P. Oleson, hep-th/9806235.
38. P. Cea and L. Cosmai, Phys. Rev. D **52**, 5152 (1995); R.W. Haymaker, hep-lat/9510035.
39. G.S. Bali, K. Schilling, and C. Schlichter, hep-lat/9802005.
40. M. Zach, M. Faber, and P. Skala, *Proc. Confinement III*, TJ Lab., 1998, hep-lat/9808055; hep-lat/9709017.
41. F. Gliozzi, in *Proc. Confinement II*, eds. N. Brambilla, G. Prosperini, (World Scientific, Singapore, 1997), hep-lat/9609040.